Egypt. J. Chem. **Vol. 65,** No. 12 pp. 11 - 19 (2022)

Egyptian Journal of Chemistry

http://ejchem.journals.ekb.eg/

Synthesis, DFT, Antibacterial and Molecular Docking Studies of Novel La(III) Complex of Benzo-Chromen Substituted Thiosemicarbazide

Eman Fares Mohamed[1]*and Safaa Said Hassan[2]*

[1]Department of Chemistry, Faculty of Science (Girls branch), Al-Azhar University, Nasr City, Egypt

[2]Department of Chemistry, Faculty of Science, Cairo University, Giza, Egypt

Abstract

1-(1-(3-oxo-3H-benzo[f]chromen-2-yl)ethylidene)thiosemicarbazide (OCETSC) and its La(III) complex was synthesized, the characterization was disbursed by elemental analysis, IR, UV–Visible, mass, magnetic measurement and molar conductance techniques. Data interpretation of the La(III) complex indicates that the complex was formed with a stoichiometric ratio of 1:2 (La: ligand). The studied ligand act as a bidentate ligand by using both azomethine nitrogen and thiol sulfur as monoanionic center of donation. The theoretical conformational structure analyses were performed using density functional theory (DFT) for ligand and complex at B3LYP functional with 6-31G(++)d,p basis set for ligand and LANL2DZ basis set for the complex. The charge distribution within the ligands and its La(III) complex was calculated using Mulliken population analysis of (MPA) and natural population analysis (NPA). The antibacterial activity of the prepared compounds was tested against some kinds of Gram-positive and negative bacteria. Molecular docking investigation proved that the ligand and complex had interesting interactions with active site amino acids of ribosyltransferase (code: 3GEY).

*Keywords:*Coumarin-yl thiosemicarbazone derivatives; La(III) complex; DFT; MPA; NPA; 3GEY.

1.Introduction

Coordination chemistry has been widely studied in lanthanide complexes, where Schiff bases ligands like thiosemicarbazones (TSCs) are accustomed to chelate individual lanthanide ions, and therefore the complexes are broadly utilized in analytical, biological, and clinical applications[1]. one among the promising areas during which these excellent metal chelators are being developed is their use as antibacterial agents. Significant progress has recently been made on these compounds which are used as drugs and possess a good range of biological activities, like antibacterial [2], antifungal [3,4], antiviral [5], antiamoebic [6], antimalarial [7], and antitumor [8] effectiveness. because the potential advantage of lanthanides continues to extend in these areas, this timely review of current applications is useful to medicinal chemists and other researchers inquisitive about the most recent developments and trends during this emerging field. Subsequently, other lanthanide-based antibacterial agents are reported, with ones featuring complexation with a wide range of ligands, including thiosemicarbazones (TSCs). Thiosemicarbazones (TSCs) are a category of Schiff bases usually obtained by the condensation of thiosemicarbazide with an appropriate aldehyde or ketone. TSCs are the main focus of chemists and biologists within the last decades on the chemistry of thiosemicarbazones (TSCs) due to their wide range of pharmacological effects to get better activity, different series of TSCs is developed by modifying the heteroaromatic system in their molecules. These compounds possessed significant biological activity when the carbonyl attachment of the side chain was located at a position α to the ring nitrogen atom, whereas attachment of the side chain β or γ to the heterocyclic N atom resulted in inactive antitumor agents. Additionally, replacement of the heterocyclic ring N with C also resulted in a biologically inactive compound suggesting that a conjugated N, N, S-tridentate donor set is crucial for the biological activities of thiosemicarbazones. Coumarin and thiosemicarbazone nuclei are the bases for

*Corresponding author e-mail: eman.fares@azhar.edu.eg (Eman F. Mohamed); hsafaa@sci.cu.edu.eg (Safaa S. Hassan)
Receive Date: 05 April 2022, Revise Date: 20 April 2022, Accept Date: 17 August 2022
DOI: 10.21608/ejchem.2022.131586.5798

several successful drugs. Coumarin compounds have quite 40 drugs, which are widely employed in medicine [9,10].

The coordination of many coumarin derivatives to the metal ions caused a great enhancement of the biological activity results as was reported in the literature [11,12]. Generally, the enhancement of the complex activity is ascribed to the synergistic impact which grows its lipophilicity [13,14]. Also, the metal thiosemicarbazone complex gives higher biological activity than the thiosemicarbazone compounds themselves. The interesting chemical properties exhibited by the complex of lanthanum metal encourage the large considerable current attention of lanthanum chemistry. So, in our work, we will describe the antibacterial effect of La-Coumarinyl thiosemicarbazone based ligand in the nanoscale to improve its effectiveness as an antimicrobial drug against different microorganisms by studying the molecular docking against the bacterial protein as Ribosyltransferase that is the target enzyme for the docking studies [15]. Finally, antiviral molecular docking will be done with the comparison theoretically between the two effects for the same compounds.

2.Experimental

2.1 Materials and reagents

$La(NO_3)_3.\ 6H_2O$ and all other chemicals were purchased from Sigma Company.

2.2 Schiff base (OCETSC) ligand and its nano La(III) - OCETSC complex preparation

1-(1-(3-oxo-3H-benzo[f]chromen-2-yl)ethylidene)thiosemicarbazide (OCETSC) ligand was synthesized in line with the known condensation method [16]. Nanostructure La-(OCETSC) complex was synthesized by pouring an ethanolic solution of nitrate salts of lanthanum (III) (1.0 mmol) into (during 20 min) an ethanolic solution of the ligand (1 mmol) under ultrasonic irradiation. After complete addition, the reaction mixture was kept in the ultrasonic bath for a period of 60 min. The obtained yellow precipitate was filtered and dried under a vacuum.

2.3 Analyses and biological measurements:

The elemental analyses were carried out by standard microanalysis techniques using automatic analyzer CHNS Vario EL III-Elementar, Germany. The conductivity meter ORION model 150 of 0.6 cells constant was used to measure the molar conductivity of the synthesized complex through the preparation of 10^{-3}M solutions using DMF as solvent. FT-IR spectra were obtained with KBr disc technique using scan Shimadzu FTIR spectrometer; the spectra were collected within the range 200-4000 cm^{-1}. The molar magnetic susceptibility of the complex was measured at temperature on prepared samples employing a magnetic susceptibility Cambridge, England Sherwood Scientific. The effective magnetic moments were calculated from the expression $\mu_{eff} = 2.828(X_M\ T)^{1/2}$ B.M., where X_M is that the molar susceptibility corrected using Parcel's constants for diamagnetism of all atoms within the compounds [17].

A modified Kirby-Bauer disc diffusion method [18] was used to determine the antimicrobial activity of the tested samples. Briefly, 100 µl of the test bacteria were grown in 10ml of Mueller Hinton media until they reached a count of roughly 10^7 cells/ml for bacteria [19] by using the plate counter. 100µl of microbial suspension was spread onto agar plates. Blank paper disks (Schleicher & Schuell, Spain) with a diameter of 8.0 mm were impregnated 10µl of testing concentration of the stock solutions and placed on agar media. Gram (+) bacteria as *Staphylococcus aureus*, *Bacillus subtilis*; Gram (-) bacteria as *Escherichia coli*, *Pseudomonas aeruginosa* were incubated at 35-37ºC for 24-48 hours. The diameters of the inhibition zones were measured in millimeters [18].

2.4 Computational methods

The input files of (OCETSC) and its La(III) complex were prepared with GaussView 5.0.8 [20]. Gaussian 09 rev. A.02 [21] was used in all calculations by the DFT/B3LYP method. 6-31G(++)d,p and LANL2DZ are the standard basis sets for the synthesized ligand and its La(III) complex respectively. All docking steps were done by MOE 2008 (Molecular Operating Environment) software to simulate the binding model of these compounds into ATP binding sites of 3GEY transferase enzyme. The protein crystal structure was obtained from the Protein Data Bank (PDB).

3.Results and discussion

3.1 Interpretation of the chemical structure:

The Elemental analyses (C, H & N) for (OCETSC) ligand and its La(III) complex show excellent comparable values between the theoretical and experimental percentage values.

A Yellowish cream precipitate was obtained; yield 80 %. For (OCETSC) $C_{16}H_{13}N_3O_2S$.(F. wt = 311.36) (Anal. Found: C, 61.20; H, 3.95; N, 12.5. Calcd: C, 61.72; H, 4.21; N, 13.5 %).

A yellow powder precipitate was obtained; yield 70 %. For $La[(C_{16}H_{12}N_3O_2S)_2\ (H_2O)_2]NO_3$.(F. wt = 857.62) (Anal. Found: C, 44.20; H, 2.95; N, 10.5. Calcd: C, 44.78; H, 3.26; N, 11.43 %). The complex

is formed with a stoichiometric ratio 1:2 (La(III): ligand).

Many pictures of La(III) complex were represented in Figure 1 that conclude the nanoscale size particles. To interpret the chemical structure of La(III)-(OCETSC) complex we discuss the following results:

First, the molar conductivity measurement pointed out that, the complex has an electrolytic nature. So, we conclude the presence of the ionic nitrate group in the outer coordination sphere of the complex as seen in the suggested chemical structure Figure 2.

Second, we confirmed the prepared La- complex by comparison between the infrared scanning of the free OCETSC ligand and its la(III) complex, we found the ligand exhibits thiol group vibration at 2676 cm^{-1} and thione band at 821 [22] indicating that it remains as the thiol-thione tautomer forms. The ligand show band at 3404 cm^{-1}, assigning the highest absorptions to υ(sym) stretching frequency for NH_2 group without any shift upon complexation in its stretching frequency meaning that the NH_2 group is still free after complexation. The disappearance of both thiol ν(SH) and thione ν(C=S) vibrations [23] upon complexation in La(III) complex can be explained in terms of coordination through the mononegatively charged sulfur atom. The clear shift of the υ (C=N) vibration to a lower value by complexation may be assigned to the coordination between the Lanthanum ion and the azomethine nitrogen. The presence of coordinated water was confirmed by the medium strength bands at 817 cm^{-1} [24]. The band positions of the carbonyl group did not change after complexation, so the carbonyl oxygen atom hasn't a role in the complexation process. New bands are formed due to (M-N), (M-O) and (M-S) bonds [25,26]. The most important characteristic bands in IR charts for both OCETSC ligand and its La-complex are listed in table 1

Third, The ^1H NMR spectrum of (OCETSC) ligand and its La(III) complex in DMSO shows signals at (OCETSC): [7.40–7.97 (5H, Ar.), 3.41(3H, methyl) ,10.54(H, NH) and 8.48(2H, NH_2)],

Fourth: The magnetic moment value of La(III) complex is 0.0 B.M. corresponding to octahedral stereochemistry with diamagnetic nature [28].

Fifth**:** The thermal stability data of the complex revealed that the first step represents the evaporation of two coordinated water molecules with a mass loss of 4.0% (calculated, 4.19%). The other mass loss is due to the decomposition of the organic ligand molecule and it is in agreement with the calculated mass loss of 37.0% (calculated, 36.6%) as mentioned in TG curve (Figure 3). The final decomposition step is represented by the total removal of the organic ligand moiety at 690 °C with the removal of the corresponding $C_{12}H_{14}N_6O_4S_2$ with a mass loss of 43.2% (calculated, 42.9%). Finally, after all decomposition steps, we found the residual elemental lanthanum product with a percent residue of 51.0 % (calculated, 50.5 %).

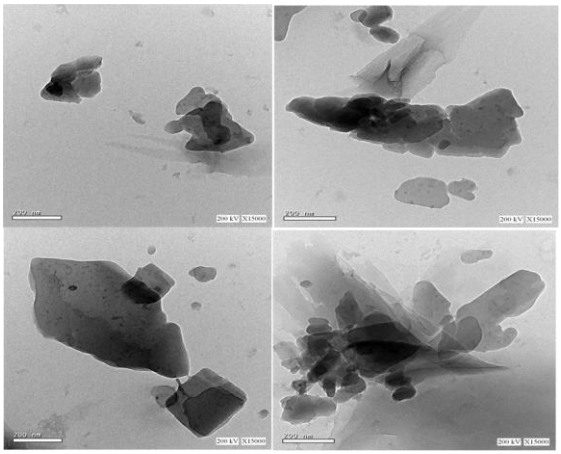

Figure 1 TEM images of synthesized La (III) complex

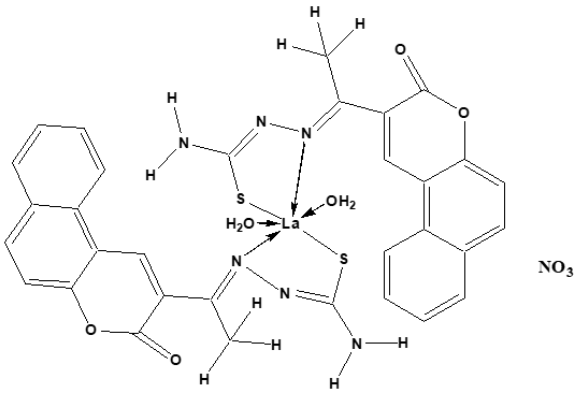

Figure 2 The suggested structure of $La[(C_{16}H_{12}N_3O_2S)_2\ (H_2O)_2]NO_3$

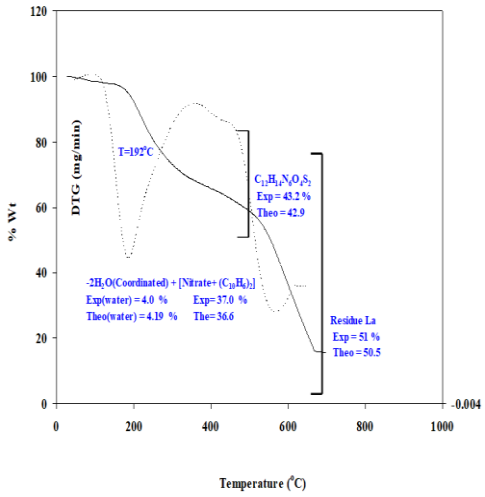

Figure 3 TG thermogram of La-(OCETSC) complex

3.2 Geometric study

The geometric optimization is carried out for the thiosemicarbazone ligand in the thiol form which was confirmed in the previous characterization part and its La(III) complex as seen in Figure 4 with the numbering system. The optimization energy, dipole moment, energy gap and hardness(η) values are mentioned in Table 2. The compound with a small HOMO-LUMO gap is reactive and is a softer molecule. As the energy gap of the studied complex decreases, the reactivity of La(III) complex increases which means that a molecule with a small HOMO-LUMO gap is more reactive and is a softer molecule. So, the reactivity and softness of the OCETSC ligand increased after its coordination to La(III) ion. The polarity of the OCETSC ligand increased after complexation by its coordination to La(III) ion as is evident from the magnitude of their dipole moments. The quantum. chemical. factors were calculated from the following equations:

$\eta = (I-A)/2$ $S= 1/ 2\eta$

$\mu = -(I +A)/2$ $\chi = (I + A)/2\eta$

$I= - E_{HOMO}$ $A= - E_{LUMO}$

Where, I = the ionization potential of the molecule

A = electron affinity of the molecule

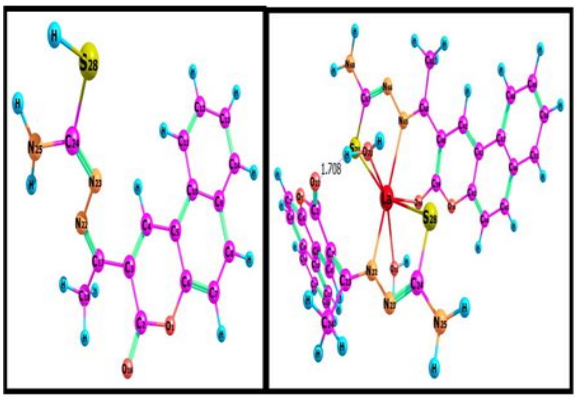

Figure 4 Optimized geometry of (OCETSC) ligand and its La(III) complex

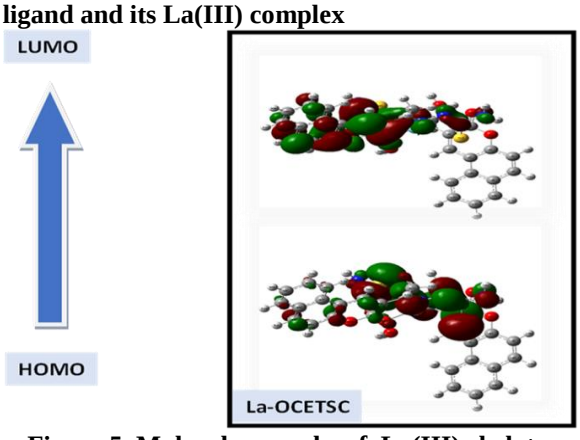

Figure 5 Molecular graphs of La(III) chelate.

The E_{HOMO} and E_{LUMO} are all negatives, representative that the products are stable. Electron density distributions of the frontier molecular orbitals (FMOs), viz the highest occupied molecular orbital (HOMOs) and lowest unoccupied molecular orbital (LUMO) of La(III) chelate are shown in Fig 5. The HOMO electron density is mainly distributed mainly over the aliphatic part of the ligand, La ion, and coordinated water molecules but in the case of LUMO, the electron density is extended to involve the whole OCETSC ligand, (the aliphatic and the aromatic rings), La ion, and coordinated water molecules.

The geometric changes that are noticed in the studied OCETSC ligand moiety itself are interesting. Thus, most of the bond lengths are increased upon complexation with the metal ion. Analysis of the data calculated for the bond lengths **(**Table 3), we can conclude that C17-N22, C24-S28, N22-N23, C24-N25, C3-C17 and C24-N23 bond lengths become longer in the complex, as the coordination takes place via N atoms of the (C=N) azomethine [29] and the sulfur of the deprotonated thiol group. This finding is due to the formation of the M-S and M-N bonds, which make the C-S and C-N bonds weaker [29]. The bond angles of the ligands are altered relatively upon coordination. The atomic charge distribution of the thiol form of the OCETSC ligand and its La(III) complex is determined by Mulliken (MPA) and natural (NPA) population analysis. The results for the selected atoms are presented in (Table 4). The distribution of positive and negative charges is important from the perspective of increase or decrease in the bond length between atoms. In the NBO analysis, the results show that the most negative atomic charges are related to nitrogen (22) atoms in the studied ligand (OCETSC) and to nitrogen and sulfur (after deprotonation) atoms in its La(III) complex. Upon chelation, the charge of the nitrogen atom has a slight decrease in its negative value with the decreasing in the remaining surrounding atoms relative to the ligand because of the involvement of the nitrogen atom in coordination to the La(III) atom with electron back–donation from the metal ion to the donating nitrogen site [30]. The cloud density on S increases after deprotonation of the thiol group with the decrease of the electron densities of the neighboring atoms because of the coordination of the sulfur atom as a mononegatively charged atom. The oxygen electron density of the water molecule was decreased upon complexation from (-0.976) to (-0.756) corresponding to the uncoordinated and the coordinated water states respectively, this is due to ligand to metal charge transfer (L→M). The electron density on La atom center increases after complexation because the charge transfer from the examined OCETSC ligand to the central La ion i.e.

L→M. So, the theoretical calculations confirm the results obtained from the analysis tools which were discussed in the previous characterization part, La(III) ion attached to the ligand via N, O (H_2O) and S donor atoms. The generated molecular orbital energy diagrams - HOMO, LUMO are presented (Figure 5).

3.3 Microbiological investigations

To assess the biological potential of the synthesized compound, the previously investigated OCETSC ligand and its La (III) complex were tested against different species of bacteria. In testing the antibacterial activity of these compounds, we used many test organisms to increase the chance of detecting antibiotic principles in testing materials. The organisms used in the present investigations included two Gram-positive (*Streptococcus mutans* and *Staphylococcus a*ureus), three Gram-negative bacteria (*Escherichia coli, Pseudomonas aeruginosa* and *klebsiella pneumonia*) and one fungi (*Candida albicans*). Gentamicin, Ampicillin and Nystatin were used as the standard drugs against the respective Gram negative, Gram positive and fungi organisms respectively. DMSO was used as control.

The outcomes of antibacterial actives in vitro of the synthesized OCETSC ligand with its La(III) complex are seen in (Table 5) and (Figure 6).

The obtained results reflect that OCETSC ligand hadn't antibacterial effect on all strains except *Escherichia coli*. We found that after complexation the antibacterial effect was generated with moderate effect against *Escherichia coli, Pseudomonas aeruginosa but* does not show any activity against *klebsiella pneumonia* from Gram negative tested, while has high antibacterial activity against *Staphylococcus a*ureus and show a non-detectible antimicrobial activity against *Streptococcus mutans* the Gram positive bacteria tested but has moderate activity against *Candida albicans*.

S. Alghool et al. and A. M. Ajlouni et al. found a similar antimicrobial effect for their lanthanide complexes to our results. The results explored high, moderate and poor antimicrobial effects.[31,32]

La(III) complex has higher antibacterial effects than (OCETSC) ligand as seen in the inhibition zone values described in (Table 5). The marked antibacterial activity results of the examined compound may be due to the chance of the formation of hydrogen bonds through the toxophorically important imine groups [(-C=N), NH_2 & oxygen water molecules] with the active center of cell constituents, thereby causing considerable interference with the normal cell process [33, 34].

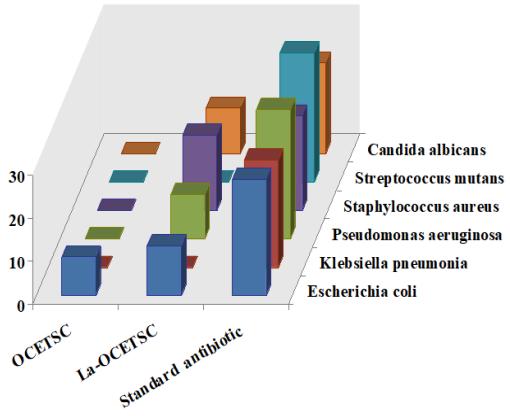

Figure 6 Biological activity of (OCETSC) ligand and its La(III) complex toward different types of bacterial strains

3.4 Docking investigations

The OCETSC ligand and its La(III) complex have interesting interactions with active site amino acids of ribosyltransferase (code: 3GEY). The $–NH_2$ amino group helped to form a backbone acceptor with Leu*A*624 and side-chain acceptor with Ser*B*514 for ligand and La-complex respectively. La-complex shows a larger number of interactions as arene-arene with Phe*A*642 and arene-cation interaction with His*B*550. Also, metal contact receptor with Lys*A*518. La- complex shows more negative scoring energy value [-5.06(RMSD=1.50)] than the OCETSC[-4.76(RMSD =2.18)] ligand itself where (RMSD) is the Root Mean Square Deviation. The different interactions were observed in Figure 7.

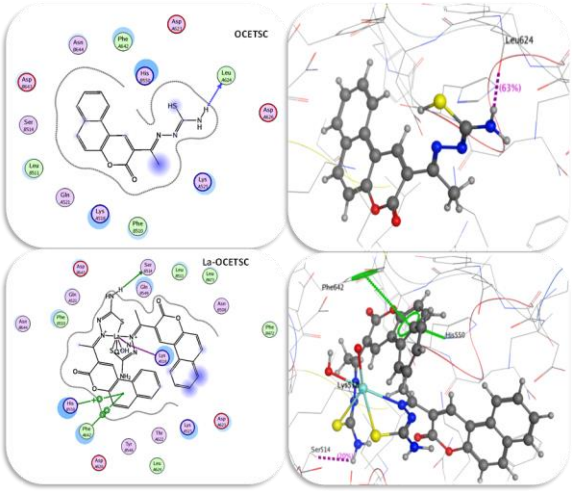

Figure **7 Docking results of (OCETSC) ligand and its La(III) complex**

(Table 1) Infrared spectral data of (OCETSC)] and its La(III) complex (cm-1).

	υ(NH_2)	υ (=C-H)	υ(-C-H)aromatic	υ (C=O)	υ (H_2O)	υ(C=N)	υ (La-N)	υ (La-O)	υ (La-S)
(OCETSC)	3404	3154	2946	1714	-----	1593	-----	-----	-----
La[(OCETSC)$_2$ (H_2O)$_2$]NO_3	3403	3172	2957	1715	817	1581	560	420	375

(Table 2) Ground state properties, HOMO–LUMO energy, hardness, ionization energy, dipole moment and electron affinity of the (OCETSC) using B3LYP/6-31G(++)d,p and La(III) complex using 3LYP/LANL2DZ.

Parameter	(OCETSC)	La[(OCETSC)2 (H2O)2]NO3
E_T, Hartree	-1330.4745	-2067.3534
E_{HOMO}, eV	-0.21775	-7.9838245
E_{LUMO}, eV	-0.09173	-5.41561263
E^*_g, eV	3.429 18	2.56821187
Hardness=1/2 (E_{LUMO}- E_{HOMO})	1.7145	1.284105935
μ, Dipole Moment (Debye)	4.9090	7.2667
I.E=- E_{HOMO}, eV	0.21775	7.983825
EA=- E_{LUMO}, eV	0.09173	5.415613

*Eg = E_{LUMO} - E_{HOMO}

(Table 3) Some of the optimized bond length, Å and bond angles, degrees, for (OCETSC) using B3LYP/6-31G(++)d,p and La(III) complex using B3LYP/LANL2DZ.

Bond length (Aº)	(OCETSC)	La[(OCETSC)$_2$ (H_2O)$_2$]NO_3
C24-S28	1.78491	1.82743
C24-N23	1.29928	1.33382
N22-N23	1.37484	1.40264
C17-N22	1.29726	1.31489
C24-N25	1.36863	1.36900
C3-C17	1.48242	1.50519
La-S28	---	2.95898
La-O31	---	2.56542
La-N22	---	2.67420
Bond angles (deg.)		
S28-C24-N23	126.201	129.622
N23-N22-C17	116.111	116.593
N22-C17-C3	115.190	118.444
N22-La-S28	---	67.695
N65-La-S71	---	67.552
N22-La-O31	---	74.609
N22-La-N65	---	154.008
S28-La-S71	---	153.235

(Table 4) Atomic charges in terms of Mulliken (MPA) and natural (NPA) population analysis of La complex of (OCETSC) using B3LYP/LANL2DZ and ligand (OCETSC) using B3LYP/6-31G(++)d,p.

Element	MPA	NPA
	La[(OCETSC)$_2$ (H_2O)$_2$]NO_3	La[(OCETSC)$_2$ (H_2O)$_2$]NO_3
La	0.119 (---)	0.244 (---)
O1	-0.276 (-0.393)	-0.543 (-0.502)
C2	0.095 (0.1732)	0.799 (0.774)
C3	0.114 (0.0200)	-0.190 (-0.189)
C4	-0.264 (0.127)	-0.099 (-0.097)

C5	0.218 (0.968)	-0.108 (-0.140)
C6	0.164 (-0.700)	0.379 (0.361)
C7	-0.380 (-0.386)	-0.236 (-0.262)
C8	-0.422 (-0.263)	-0.157 (-0.175)
C9	0.387 (0.283)	-0.061 (-0.066)
C10	0.146 (1.016)	-0.022 (-0.019)
O16	-0.232 (-0.419)	-0.583 (-0.574)
C17	0.167 (-0.220)	0.359 (0.255)
C18	-0.697 (-0.489)	-0.675 (-0.709)
N22	-0.176 (-0.290)	-0.283 (-0.315)
N55	-0.117 (---)	-0.250 (---)
N23	-0.013 (-0.115)	0.417 (-0.422)
C24	-0.119 (-0.018)	0.357 (0.281)
N25	-0.574 (-0.350)	-0.829 (-0.848)
S28	0.013 (0.059)	-0.124 (-0.008)
S61	-0.011 (---)	-0.065 (---)
O31(H_2O)	-0.734 (---)	-0.945 (---)
Cl	-0.244 (---)	-0.361 (---)
Br13	--- (---)	--- (---)
C11	-0.372 (-0.335)	-0.194 (-0.207)
C12	-0.259 (-0.301)	-0.195 (-0.223)
C13	-0.170 (-0.182)	-0.211 (-0.238)
C14	-0.419 (-0.162)	-0.189 (-0.201)

(Table 5) Antibacterial activity data of (OCETSC) ligands and its La(III) complex, inhibition zone (mm

Inhibition zone diameter(mm/mg sample)				
Sample / Microorganism	**Control: DMSO**	**(OCETSC)**	La[(OCETSC)$_2$(H_2O)$_2$]NO_3	Standard antibiotic
Gram negative bacteria				Gentamicin
Escherichia coli	0.0	9	11.6±0.5	27±0.5
Klebsiella pneumonia	0.0	0.0	0.0	25±0.5
Pseudomonas aeruginosa	0.0	0.0	10.3±0.5	30±0.5
Gram positive bacteria				Ampicillin
Staphylococcus aureus	0.0	0.0	17.6±0.6	22±0.1
Streptococcus mutans	0.0	0.0	0.0	30±0.5
Fungi				Nystatin
Candida albicans	0.0	0.0	10.6±0.5	21±0.5

4. Conclusions

The antibacterial behaviour of the benzo chromene derivative ligand [1-(1-(3-oxo-3H-benzo[*f*]chromen-2-yl)ethylidene)thiosemicarbazide (OCETSC)] was improved after its chelation to la lanthanide metal ion. The structure of La(III) complex was interpreted by physicochemical tools. It was found that the ligand is a uninegatively bidentate ligand, attached to La(III) ion as 1:2 (M:L) complex via azomethine N and deprotonated thiol S with the formation of distorted octahedral structure. DFT calculation was carried out for the prepared ligand and its La(III) complex with the calculation of charge distribution within the ligand and its La(III) complex using Mulliken population analysis (MPA) and natural population analysis (NPA). The docking simulation pointed out the binding model of (OCETSC) as free ligand and as La(III) complex. The interactions with active site amino acids of ribosyltransferase (code: 3GEY) involved the hydrogen bond formation and arene-arene interaction. So, the current findings provide a new chance for the development and discovery of novel antimicrobials to beat the ever increasing drug resistance problem.

5. Conflicts of interest

There are no conflicts to declare.

6. References:

1. E. M. Abdalla, S. S. Hassan, H. H. Elganzory, S. A. Aly, H. Alshater, J. Molecules, 2021, 26, 19, 5851.
2. R. Ramachandran, M. Rani, S. Kabilan, *Bioorg. Med. Chem. Lett.* 2009, *19*, 2819.
3. D. K. Demertzi, J. R. Miller, N. Kourkoumelis, S. K. Hadjikakou, M. A. Demertzis, Polyhedron. 1999, *18*, 1005.
4. R.A. Finch, M. C. Liu, S.P.Grill, W.C. Rose, R.Loomis, K.M. Vasquez, Y. C. Cheng, A.C. Sartorelli. Biochem. Pharmacol. 2000, *59*, 983.
5. S. Sharma, F. Athar, M.R. Maurya, A. Azam, Eur. J. Med. Chem. 2005, *40*, 1414.
6. G.L. Parrilha, J.G. da Silva, L.F. Gouveia, A.K. Gasparoto, R.P. Dias, W.R. Rocha, D.A. Santos, N.L. Speziali, H. Beraldo. Eur. J. Med. Chem. 2011, *46*, 1473.
7. K. Alomar, V. Gaumet, M. Allain, G. Bouet, A. Landreau, J. Inorg. Biochem. 2012, *115*, 36.
8. A. Usman, I.A. Razak, S. Chantrapromma, H. K. Fun, A. Sreekanth, S. Sivakumar, M. Prathapachandra Kurup, Acta Crystallogr., Sect. C: Cryst. Struct. Commun. 2002, *58*, 461.
9. F. A. Jimenez-Orozco, J. A. Molina-Guarneros, N. Mendoza-Patino, F. Leon- Cedeno, B. Flores-Perez, E. Santos-Santos, J.J. Mandoki, Melanoma Res. 1999, 9, 243.
10. G. J. Finn, B. S. Creaven, D. A. Egan, Melanoma Res. 2001,11, 461.
11. K. B. Gudasi, R.V. Shenoy, R. S. Vadavi, M. S. Patil and S. A. Patil, *Chem. Pharm. Bull.* 2005, 53, 1077.
12. I. Kostova, G. Momekov, M. Zaharieva and M. Karaivanova, Eur. J. Med. Chem. 2005, 40, 542.
13. S. S. Kukalenko, B. A. Borykin, S. I. Sheshtakova and A. M. Omelchenko, Russ. Chem. Rev. 1985, 54, 676.
14. M. S. Refat, I. M. El-Deen, Z. M. Anwer and S. El-Ghol, J. Molec. Struc. 2009, 920, 149.
15. S. S. Hassan, S. M. Gomha, Chemical Papers, 2018, 73, 2, 331.
16. R. J. Fessenden and J. S. Fessenden, 4th.ed, Inorg. Chem., Cole Publishing Company, California, 1990, 13, 587.
17. H. J. Emeleus and A. G. Sharpe, 4th ed., London, 1974.
18. National Committee for Clinical Laboratory Standards. Reference Methods for broth dilution antifungal susceptibility testing of conidium- forming filamentous fungi:proposed standard M38-A. NCCLS, wayne, PA, USA, 2002.
19. National Committee for Clinical Laboratory Standards. Method for antifungal disk diffusion susceptibility testing of yeast: proposed guideline M44-P, NCCLS, Wayne, PA, USA, 2003.
20. GaussView 5.0, (Gaussian Inc.,Wallingford, CT, USA), 2009.
21. Gaussian 09 rev. A.02, (Gaussian Inc.,Wallingford, CT, USA), 2009.
22. S. S. Hassan, Antibacterial, DFT and molecular docking studies of Rh(III) complexes of Coumarinyl-Thiosemicarbazone nuclei based ligandsJ. Appl Organometal Chem. 2017, 3, 32.
23. K. Nakamoto, 4th ed., Wiley-Interscience, New York, 1986.
24. M. L. Dianui, A. Kriza, N. Stanica and A. M. Musuc, *J. Serb. Chem. Soc*. 2010, 75, 1515.
25. H. A. Qaseer, Croat. Chem. Acta 2005, 78, 79.
26. M. A. Behtnett, R. J. H. Clark, and D. L. Milner, Inorg. Chem. 1967, 9.
27. S. S. Hassan, M. M. Shoukry, R. N. Shallan and R. van Eldik, J. Coord. Chem. 2017,70, 1761.
28. C. L. Jain and B. L. Khandelwal, J. inorg. nucL. Chem. 1980, 42, 1769.
29. O. A. El-Gammal, Spectrochim. Acta A 2010, 75, 533.
30. M. Naseh, T. Sedaghat, A. Tarassoli and E. Shakerzadeh, Comput. Theor. Chem. 2013, 1005, 53.
31. S. Alghool, H. F. Abd El-Halim, M. S. Abd El-sadek, I. S. Yahia,L. A. Wahab, J. Therm. Anal. Calorim. 2013, 112, 671.
32. A. M. Ajlouni, Q. Abu-Salem, Z. A. Taha, A. K. Hijazi, W. Al Momani,J Rare Earth 2016, 34, 986.
33. A. A El-Sherif, M. M Shoukry, J. Inorg. Chim. Acta 2007, 360, 473.
34. A. T. Abdelkarim, J. Pharm. Sci. 2015, 5, 839.
35. M. Carcelli, P. Mazza, C. Pelizzi, G. Pelizzi, F. Zani, J. Inorg. Biochem. 1995, 57, 43.
36. O. William and F. Febrzldry, J. Pharm. Sci. 1961, 50.
37. G. L. Parrilha, J. G. da Silva, L. F. Gouveia, A. K. Gasparoto, R. P. Dias, W. R. Rocha, D. A

Santos, N. L. Speziali and H. Beraldo, Eur. J. Med. Chem. 2011, 46, 1473.